

Importance of local structures of second and third repeat fragments of microtubule-binding domain for tau filament formation

Mari Tokimasa^a, Katsuhiko Minoura^a, Shuko Hiraoka^a, Koji Tomoo^{a,*}, Miho Sumida^b, Taizo Taniguchi^b, Toshimasa Ishida^a

^a Department of Physical Chemistry, Osaka University of Pharmaceutical Sciences, 4-20-1 Nasahara, Takatsuki, Osaka 569-1094, Japan

^b Hyogo Institute for Aging Brain and Cognitive Disorders, 520 Saisho-ko, Himeji, Hyogo 670-0981, Japan

Received 5 January 2005; revised 29 April 2005; accepted 4 May 2005

Available online 1 June 2005

Edited by Jesus Avila

Abstract To investigate the importance of the seventh residue of the second and third repeat fragments (R2 and R3 peptides) of the microtubule-binding domain (MBD) for tau filamentous assembly, the residues Lys and Pro were substituted (R2-K7P and R3-P7K). The filament formations of the R2 and R3 peptides were almost lost due to their substitutions despite their overall conformational similarities. The NOE analyses showed the importance of the conformational flexibility for the R2 peptide and the coupled extended and helical conformations for the R3 peptide in their limited N-terminal regions around their seventh residues. The result shows that the filament formation of MBD is initiated from a short fragment region containing the minimal conformational or functional motif.

© 2005 Federation of European Biochemical Societies. Published by Elsevier B.V. All rights reserved.

Keywords: Tau protein; Microtubule-binding domain; Filament formation; Conformation

1. Introduction

The microtubule (MT)-associated protein tau is an important component of the neuronal cytoskeleton and plays a role in the formation and stabilization of MTs. The tau protein is a highly soluble protein with a random conformation and shows almost no tendency to aggregate under physiological conditions. Many neurodegenerative diseases, however, are characterized by the abnormal aggregation of this tau protein into an insoluble paired helical filament (PHF), the major component of the neurofibrillary tangles (NFTs). In the brains of Alzheimer's disease (AD) patients, the tau protein dissociates from axonal MTs through an extensive phosphorylation and abnormally aggregates itself to form the insoluble NFT (reviewed in [1–5]). Since the degree of dementia in AD patients significantly correlates with the appearance and distribution of this tangle [6], it is of importance for the prevention and medica-

tion of AD to find a method of inhibiting such an abnormal aggregation of the tau protein.

The tau protein binds to MTs through the MT-binding domain of the three- or four-repeat sequence located in the C-terminal half (Fig. 1) [2,3]. Although the structural details of the tau protein self-assembly are yet to be completely elucidated, it was clarified that the core structure of PHF is mainly composed of the microtubule-binding domain (MBD) [7], which promotes the tau protein assembly in vitro [8]. Recently, we have reported that the in vitro filament formation of four-repeat MBD is mainly promoted by the second and third repeat fragments (R2 and R3), and their filament formation properties are considerably different in points, such as speed, optimal trifluoroethanol (TFE) content, and process for heparin-induced filament formation [9–11]. Also, we determined the conformations of the R2 and R3 peptides in TFE solution and found that the R3 peptide shows amphipathic extended and α -helical structures at the N-terminal Val1-Lys6 and Leu10-Leu20 sequences, respectively, whereas the averaged backbone conformation of the R2 peptide shows an amphipathic α -helical structure at the Ile3-His25 sequence [10,12,13]; von Bergen et al. [14] also reported that this VQIVYK local sequence of the R3 repeat (Fig. 1) plays an important role in the aggregation of the tau protein into Alzheimer's PHF. As the R2 and R3 peptides are both composed of similar amino acid sequences, it can be considered that some specific amino acid residues in their repeat peptides cause such a different conformation/aggregation property.

The main reason the extended structure is formed at the N-terminal region of the R3 peptide, but not of the R2 peptide, could be the presence of the Pro residue at the seventh position. Therefore, as part of a series of studies attempting to clarify residues responsible for the filamentous assemblies characteristic of the R2 and R3 peptides, their seventh residues, Lys and Pro, were substituted (R2-K7P and R3-P7K) (Fig. 1). In this paper, we report their filament formation and conformation characteristics, investigated by the CD, ThS fluorescence and ¹H NMR measurements.

2. Materials and methods

2.1. Chemicals and peptides

Heparin (average molecular weight, 6000) and thioflavin S (ThS) were obtained from Sigma Co. The R2 and R3 peptides and their substitutes (R2-K7P and R3-P7K) were synthesized using a solid-phase

*Corresponding author. Fax: +81 72 690 1068.

E-mail address: tomoo@gly.oups.ac.jp (K. Tomoo).

Abbreviations: AD, Alzheimer's disease; MBD, microtubule-binding domain; MT, microtubule; NFT, neurofibrillary tangle; NOESY, nuclear Overhauser effect spectroscopy; NOE, nuclear Overhauser effect; PHF, paired helical filament; TFA, trifluoroacetic acid; TFE, trifluoroethanol; ThS, thioflavin S; TOCSY, total correlation spectroscopy; TSP, 3-(trimethylsilyl)propionic acid

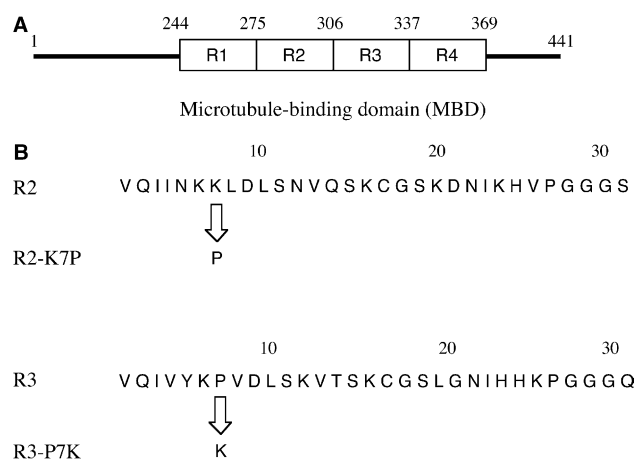


Fig. 1. (A) Schematic diagram of entire human four-repeat tau protein and (B) R2 and R3 peptides corresponding to second and third fragments of four-repeat MBD. In the R2-K7P and R3-P7K peptides, the seventh residue positions of R2 and R3 peptides are substituted for Pro and Lys residues, respectively. The regions from the first to the fourth MBD repeats in (A) are represented by R1–R4, respectively. The numbering of the amino acid residues refers to the longest isoform of human tau (441 residues).

peptide synthesizer. These peptides were characterized by mass spectrometry and determined to be >95.0% pure by reverse-phase HPLC. The peptides were obtained in the form of lyophilized powder (including trifluoroacetic acid as counterion).

2.2. CD measurements

Each peptide was adjusted to 40 μM in water, TFE, or their mixture of different ratio, in which the pH was adjusted to 4.0 by adding HCl or NaOH. All measurements were carried out at 25 $^{\circ}\text{C}$ with a JASCO J-820 spectrometer in a cuvette with a 2 mm path length. For each experiment under N_2 gas flow, the measurement from 190 to 260 nm was repeated eight times and the results were summed. Then, the molar ellipticity was determined after normalizing the peptide concentration. The same experiment was performed at least three times using freshly prepared samples, and average values are presented in this paper. Data are expressed as mean residue ellipticity $[\theta]$ in $\text{deg cm}^2 \text{dmol}^{-1}$.

2.3. ThS fluorescence intensity measurements

The concentration of each peptide was adjusted to 15 μM using 50 mM Tris-HCl buffer (pH 7.5) containing 10 μM ThS dye. It was reported that thioflavin dyes such as ThS can be used to quantify filament formation in solution [15]. Aggregation was induced by adding 3.8 μM heparin to the solution prior to ThS fluorescence intensity measurement. Fluorescence intensity was measured using a JASCO FP6500 instrument with a 2-mm quartz cell, whose temperature was maintained at 25 $^{\circ}\text{C}$ by a circulating water bath. The aggregation kinetics was analyzed by recording the time-dependent change of ThS fluorescence intensity at an excitation of 440 nm and an emission of 490 nm. The background fluorescence intensity of each peptide was subtracted when required.

2.4. ^1H NMR measurements

Each peptide was used without further purification by dissolving in water/TFE- d_2 mixture to prepare a sample solution of 1–2 mM concentration (20% and 100% TFE for the R2 and R2-K7P peptides, and 0%, 40% and 100% TFE for the R3 and R3-P7K peptides). ^1H NMR spectra were recorded using a Varian unity INOVA500 spectrometer with a variable temperature-control unit. The ^1H chemical shifts were referenced to 0 ppm for 3-(trimethylsilyl)propionic acid (TSP). The conventional NMR measurement was performed at 298 K. Two-dimensional total correlation spectroscopy (TOCSY) and nuclear Overhauser effect spectroscopy (NOESY) spectra were acquired in a phase-sensitive mode using standard pulse programs available in the Varian software library. The proton peaks of the R2-K7P and R3-P7K peptides were assigned by referring to the previous

reports of the R2 and R3 peptides in TFE [10,12]. Assuming the same correlation time for all the protons, the offset dependence of NOESY cross peaks was used for the estimation of the secondary structure of the peptide, by which NOE intensities were classified into three categories (strong, medium, and weak).

3. Results and discussion

3.1. Conformational similarity between R2 and R3-P7K peptides and between R3 and R2-K7P peptides

To investigate the effect of the substitution of the seventh residue on the overall conformations and flexibilities of the R2 and R3 peptides, their CD spectra were measured as a function of TFE content. The results for the R2-K7P and R3-P7K peptides are shown in Fig. 2; those for R2 and R3 were previously reported [10,12]. Although the quantification of CD spectra in terms of secondary structure components is often unreliable, the spectra are useful to estimate the gross conformational state. The CD spectra of all the peptides in water predominantly showed a random conformation characterized by a negative peak at approximately 197 nm, whereas the spectra in 100% TFE were indicative of an α -helical structure characterized by two negative peaks at approximately 209 and 222 nm. Detectable conformational transitions were observed when the peptides were dissolved in an approximately 20% TFE solution, and the conformations of α -helical structures consistently increased in proportion to the TFE content. Since these CD spectral changes were completely reversible and no notable lag times were observed, it could be stated that the transitions between the random and helical conformations of these peptides are sufficiently flexible and the peptides change their conformations easily, depending on the hydrophobic and hydrophilic balance of the solvent.

On the other hand, the TFE content-dependent profiles of α -helical content (Fig. 2C), calculated from the CD ellipticity at 222 nm [16], showed a marked resemblance between the R3 and R2-K7P peptides and between the R2 and R3-P7K peptides, where the molar ellipticities of the former peptides are considerably larger than those of the latter peptides. This indicates that the overall conformational and transitional characteristics of the R2 and R3 peptides are highly dominated by their seventh residues.

3.2. TFE content-dependent aggregation profiles of R2 and R3 peptides

The heparin-induced filament formation characteristics of the R2 and R3 peptides and their substitution peptides were investigated on the basis of their reaction time – ThS fluorescence intensity profiles in the aqueous solutions of different TFE contents. Consequently, it was shown that the TFE contents of 20% and 40% are optimal for the effective filament formations of the R2 and R3 peptides, respectively (Fig. 3). The R2 or R3 peptide in the aqueous solution of this optimal TFE content is in an intermediate transition state from a random structure to an α -helical structure, as is obvious from their CD spectral changes (Fig. 2C). Since the increase of ThS fluorescence is considerably inhibited in an aqueous solution of <10% or >60% TFE [10], this result indicates that such an intermediate conformation is the most likely factor responsible for the filament formations of the R2 and R3 peptides.

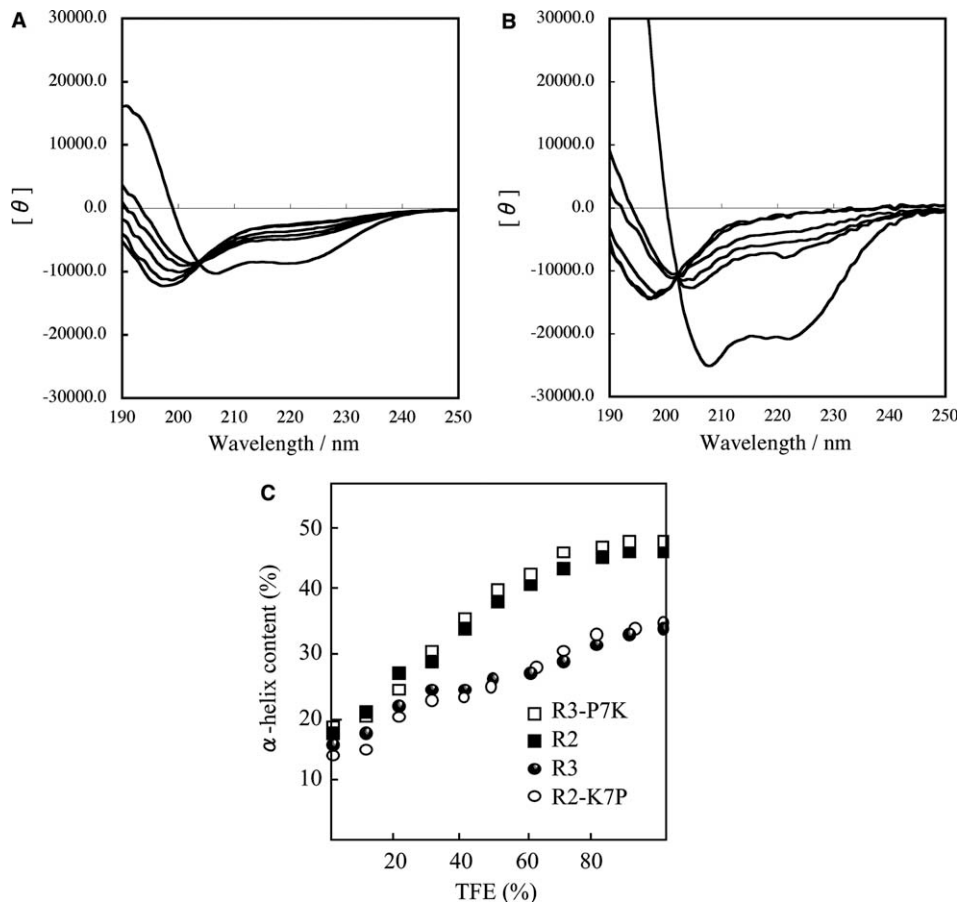


Fig. 2. CD spectra of R2-K7P (A) and R3-P7K (B) peptides, and α -helical contents of R2, R2-K7P, R3, and R3-P7K peptides at different water/TFE ratios (C). Curves of (A) and (B) from top to bottom at the 210–230 nm region were spectrally measured at 0%, 10%, 20%, 30%, 50% and 100% TFE.

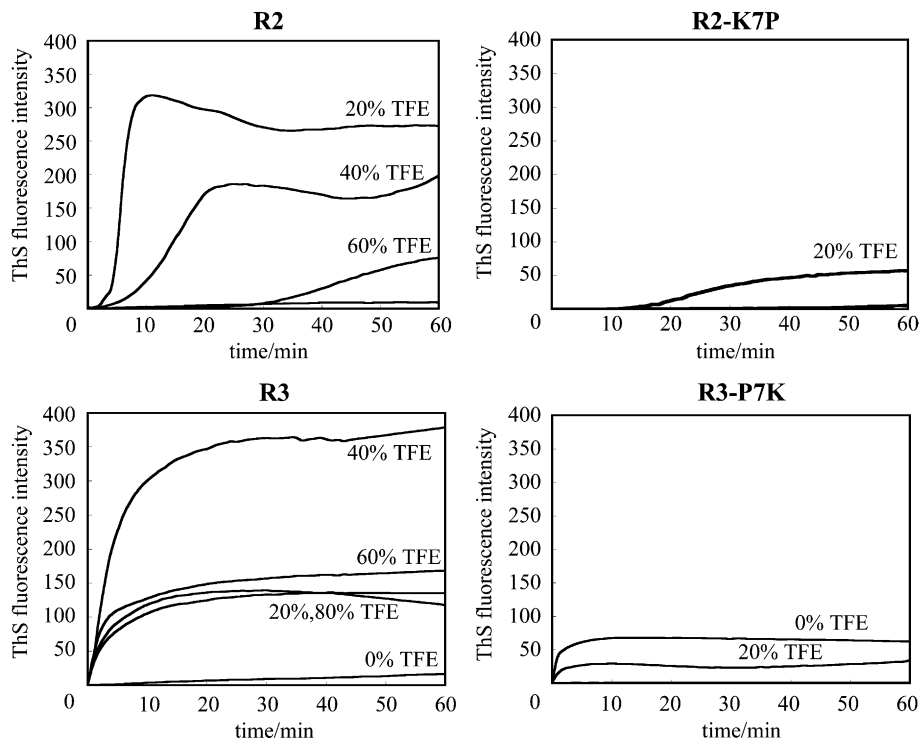


Fig. 3. Reaction time – ThS fluorescence profiles of R2, R2-K7P, R3, and R3-P7K peptides at different water/TFE ratios.

In contrast, the TFE content-dependent filament formation abilities of the R2 and R3 peptides were almost lost by the substitutions of their seventh residues. The R2-K7P and R3-P7K peptides showed neither the notable filament formation nor the TFE content dependency, suggesting that the Lys and Pro residues of the R2 and R3 peptides in MBD are crucial to the PHF filament formation of the tau protein.

On the other hand, it is interesting to note that the filament of the R3-P7K peptide, although less extensive, was best formed in water, but not in 40% TFE (=optimal content for the R3 peptide), whereas the R2-K7P peptide still showed the same TFE content-dependent filament formation as the R2 peptide (optimal TFE = 20%). This indicates that the conformations of the R2-K7P and R3-P7K peptides suitable for filament formations are different from each other.

3.3. NOE connectivity between neighboring protons of N-terminal region in optimal TFE solution

The CD and fluorescence spectral results suggested that a transition conformation from the random structure to the α -helical-like structure, particularly regarding the N-terminal region containing the seventh residue, could be the most likely factor responsible for the filament formations of the R2 and R3 peptides. To investigate their conformational features responsible for the filament formations, the NOE connectivities of neighboring protons were compared between the R2 and R2-K7P peptides in 20% and 100% TFE solutions and between the R3 and R3-P7K peptides in 0%, 40% and 100% TFE solutions. The sequential NOE networks of the N-terminal moieties along the peptide backbone protons are shown in Figs. 4 and 5; the results of the R2 and R3 peptides in 100% TFE were already reported [10,13], and no notable differences were observed between the NOE connectivities of R2 and R3 peptides and their substituted ones at their central and C-terminal regions (data not shown).

As for the R2 and R2-K7P peptides, the fastest filament formations were both observed in 20% TFE solution, although their degrees are largely different. Therefore, the NOE patterns commonly observed (Fig. 4A) would be responsible for the filament formation, i.e., two NOE-connected segments at the N-terminal region. Since it is known that the extended and helical structures of peptide backbone

are directly related to the $d_{\alpha\text{N}(i,i+1)}$ and $d_{\text{NN}(i,i+1)}$ NOE intensities, respectively, it would say that the VQIIN and KLD fragments correspond to the regions of taking the high conformational flexibilities and that the decreased filament formation of the R2-K7P peptide is due to the partial limitation of these conformational flexibilities by the substitution of Pro residue. In this regard, the basic KK sequence of the R2 peptide may be important for accelerating the acidic heparin-induced filament formation. On the other hand, the NOE patterns in 100% TFE (Fig. 4B) showed the different conformations of both peptides at the N-terminal regions, i.e., an α -helical conformation and an extended structure of the R2 and R2-K7P peptides, respectively. Since neither peptide in 100% TFE solution showed any filament formation, this means that the TFE-induced stable secondary structure such as a typical helix or sheet structure is not suitable for the filament formation of the R2 peptide.

The NOE connectivities of the R3 and R3-P7K peptides in 0%, 40% and 100% TFE solutions are shown in Fig. 5. The ThS fluorescence measurement (Fig. 3) showed that, although the filament formation of the R3 peptide is optimal in 40% TFE solution, the filament is still positively formed in 80% TFE, as compared with that in water. Since the NOE network of the R3 peptide in 100% TFE was almost the same as that of 80% TFE (data not shown) and is similar to that of 40% TFE, it would say that the TFE-induced stable conformation of R3 peptide is a suitable form for the filament formation, i.e., the coupled conformation of an extended VQIVYK structure and a helical LSK structure (continuing to Leu20) at the N-terminal moiety [10], and this is in contrast with the case of R2 peptide. On the other hand, the R3-P7K peptide did not show such a TFE-independent conformational feature, and the N-terminal conformation is considerably dependent on the TFE content. The filament formation observed in water may result from a relatively rigid and long-range extended structure, and the basic Lys-Lys sequence may play an important role in the heparin-induced filament formation.

On the basis of the conformational differences between the R2 and R3 peptides and their substituted peptides, it would be possible to discuss the relationship between the conformational features and the filament formations of these peptides. The NOE results showed that the break of the high flexible

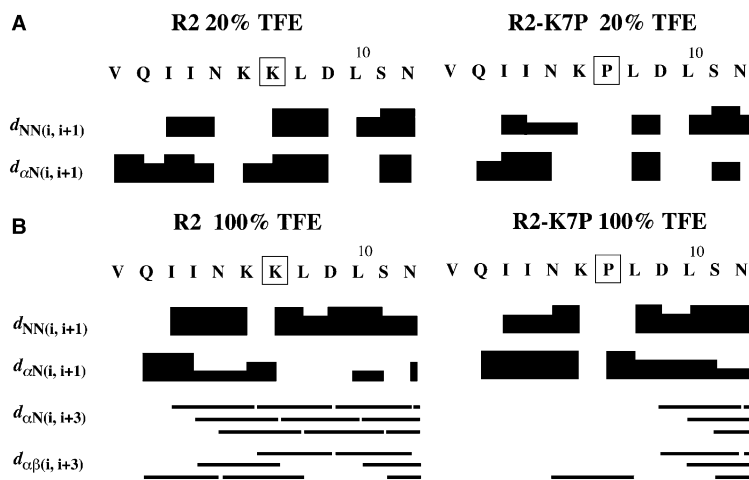


Fig. 4. Diagrams of NOE connectivity between neighboring protons along backbone chain of R2 and R2-K7P peptides ($d_{\alpha\text{N}(i,i+1)}$, $d_{\text{NN}(i,i+1)}$, $d_{\alpha\text{N}(i,i+3)}$ and $d_{\alpha\text{B}(i,i+3)}$) in 20% TFE (A) and 100% TFE (B). Observed NOE intensities are indicated by the thickness of each bar.

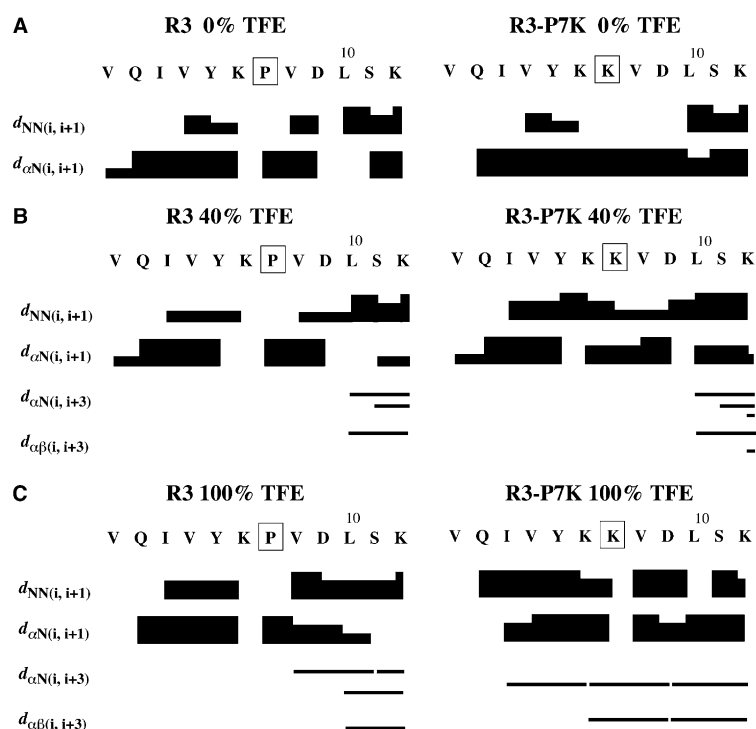


Fig. 5. Diagrams of NOE connectivity between neighboring protons along backbone chain of R3 and R3-P7K peptides ($d_{\alpha N(i, i+1)}$, $d_{NN(i, i+1)}$, $d_{\alpha N(i, i+3)}$ and $d_{\alpha\beta(i, i+3)}$) in water (A), 40% TFE (B) and 100% TFE (C) solutions. Observed NOE intensities are indicated by the thickness of each bar.

and random structures at the Gln2-Asn5 and Lys7-Asp9 sequences, caused by the Lys \rightarrow Pro substitution at the seventh position, leads to a considerable decrease in the TFE-dependent filament formation ability of the R2 peptide, suggesting the importance of the conformational flexibility of these N-terminal regions for the filament formation. In contrast, the TFE-independent Val1-Lys6 extended and Leu10-Leu20 helical structures were shown to be necessary for an effective filament formation of the R3 peptide. The break of these coupled secondary structures at the N-terminal region by the Pro \rightarrow Lys substitution leads to a marked decrease in the filament formation.

In conclusion, the present study clarified the importance of the seventh residues for the filament formations of the R2 and R3 repeat fragments of MBD, although their accurate functions have not yet been clarified. Furthermore, an important insight obtained from this work is that the filament formation of MBD could be largely dependent on a short fragment containing the minimal conformational or functional motif for forming the core of filament, namely the high flexibility of the R2 fragment and the coupled extended and helical structures of the R3 fragment in their limited N-terminal regions around their seventh residues.

References

- [1] Buee, L., Bussiere, T., Buee-Scherrer, V., Delacourte, A. and Hof, P.R. (2000) Tau protein isoforms, phosphorylation and role in neurodegenerative disorders. *Brain Res. Rev.* 33, 95–130.
- [2] Goedert, M. and Spillantini, M.G. (2000) Tau mutations in frontotemporal dementia FTDP-17 and their relevance for Alzheimer's disease. *Biochim. Biophys. Acta* 1502, 110–121.
- [3] Friedhoff, P., von Bergen, M., Mandelkow, E.-M. and Mandelkow, E. (2000) Structure of tau protein and assembly into paired helical filaments. *Biochim. Biophys. Acta* 1502, 122–132.
- [4] Garcia, M.L. and Cleveland, D.W. (2001) Going new places using an old MAP: tau, microtubules and human neurodegenerative disease. *Curr. Opin. Cell. Biol.* 13, 41–48.
- [5] Lee, V.M., Goedert, M. and Trojanowski, J.Q. (2001) Neurodegenerative tauopathies. *Annu. Rev. Neurosci.* 24, 1121–1159.
- [6] Arriagada, P.V., Growdon, J.H., Hedley-Whyte, E.T. and Hyman, B.T. (1992) Neurofibrillary tangles but not senile plaques parallel duration and severity of Alzheimer's disease. *Neurology* 42, 631–639.
- [7] Friedhoff, P., von Bergen, M., Mandelkow, E.-M. and Mandelkow, E. (1998) A nucleated assembly mechanism of Alzheimer paired helical filaments. *Proc. Natl. Acad. Sci. USA* 95, 15712–15717.
- [8] Wille, H., Drewes, G., Biernat, J., Mandelkow, E.-M. and Mandelkow, E. (1992) Alzheimer-like paired helical filaments and antiparallel dimers formed from microtubule-associated protein tau in vitro. *J. Cell. Biol.* 118, 573–584.
- [9] Yao, T.-M., Tomoo, K., Ishida, T., Hasegawa, H., Sasaki, M. and Taniguchi, T. (2003) Aggregation analysis of the microtubule binding domain in tau protein by spectroscopic methods. *J. Biochem.* 134, 91–99.
- [10] Minoura, K., Yao, T.-M., Tomoo, K., Sumida, M., Sasaki, M., Taniguchi, T. and Ishida, T. (2004) Different associational and conformational behaviors between the second and third repeat fragments in the tau microtubule-binding domain. *Eur. J. Biochem.* 271, 545–552.
- [11] Hiraoka, S., Yao, T.-M., Minoura, K., Tomoo, K., Sumida, M., Taniguchi, T. and Ishida, T. (2004) Conformational transition state is responsible for assembly of microtubule-binding domain of tau protein. *Biochem. Biophys. Res. Commun.* 315, 659–663.
- [12] Minoura, K., Tomoo, K., Ishida, T., Hasegawa, H., Sasaki, M. and Taniguchi, T. (2002) Amphipathic helical behavior of the third repeat fragment in the tau microtubule-binding domain,

- studied by ^1H NMR spectroscopy. *Biochem. Biophys. Res. Commun.* 294, 210–214.
- [13] Minoura, K., Tomoo, K., Ishida, T., Hasegawa, H., Sasaki, M. and Taniguchi, T. (2003) Solvent-dependent conformation of the third repeat fragment in the microtubule-binding domain of tau protein, analyzed by ^1H -NMR spectroscopy and molecular modeling calculation. *Bull. Chem. Soc. Jpn.* 76, 1617–1624.
- [14] von Bergen, M., Friedhoff, P., Biernat, J., Heberle, J., Mandelkowitz, E.M. and Mandelkowitz, E. (2000) Assembly of tau protein into Alzheimer paired helical filaments depends on a local sequence motif ((306)VQIVYK(311)) forming beta structure. *Proc. Natl. Acad. Sci. USA* 97, 5129–5134.
- [15] Friedhoff, P., Schneider, A.E.M., Davies, P. and Mandelkowitz, E. (1998) Rapid assembly of Alzheimer-like paired helical filaments from microtubule-associated protein tau monitored by fluorescence in solution. *Biochemistry* 37, 10223–10230.
- [16] Chen, Y.H., Yang, J.T. and Martinez, H.M. (1972) Determination of the secondary structures of proteins by circular dichroism and optical rotatory dispersion. *Biochemistry* 11, 4120–4131.